

EXPERIMENTS IN PRECISION COMMON TIME FOR MOBILE PLATFORMS

John B. Lundberg
Naval Surface Warfare Center Dahlgren
Joint Fires and Space Applications
Suite 336, RM 2080, 19008 Wayside Dr.
Dahlgren VA 22448-5162, USA
Tel: (540) 653-1336

James P. Cunningham
Naval Surface Warfare Center Dahlgren
Joint Fires and Space Applications
Suite 336, RM 2080, 19008 Wayside Dr.
Dahlgren VA 22448-5162, USA
Tel: (540) 653-8406

Abstract

Various naval applications can benefit from the synchronization of clocks across mobile platforms, particularly if the time synchronization is accomplished at the few-nanosecond level. The Naval Surface Warfare Center, Dahlgren Division, has undertaken the task of merging precise point positioning capabilities with common view mode techniques to demonstrate the capability of determining relative clock offsets in real time to the nanosecond level for clocks on mobile platforms. These demonstrations compare the GPS-derived clock offsets between the USNO Master Clock and a portable rubidium clock that supports an Ashtech Z12-T and is carried in a van that is located approximately 60 km from USNO. The data are postprocessed as if they were collected and processed in real time. The Kalman filter estimates of the relative clock offsets are compared to the measured clock offsets that are determined by comparing the rubidium clock to a portable cesium clock that was synchronized with the USNO Master Clock. After adjustment for a system bias, the estimated clock offsets agree with the measured clock offsets to the few-nanosecond level. These demonstrations have provided the incentive for integrating this capability with various measurement systems that could benefit from this level of clock synchronization.

INTRODUCTION

The capability to synchronize clocks on two or more mobile platforms in real-time or near real-time can be utilized by various systems to improve their performance or capabilities, particularly if the synchronization can be accomplished at the few-nanosecond level. Experiments were conducted at the Naval Support Facility Dahlgren (NSFD) to evaluate the use of a Global Positioning System (GPS)-based

precise point positioning (PPP) technique [1,2] and the common view mode (CVM) technique [3] in achieving nanosecond-level clock synchronization for baseline distances of approximately 60 km for a mobile platform. The basic assumption in these experiments is that GPS data are consistently available to the platforms along with precise estimates of the orbit and clock states of the GPS satellites, thus permitting reliable PPP solutions at the 10-30 cm level. A platform's GPS data would first be used in the PPP solutions and then the PPP solutions and GPS data would be used to determine platform clock offsets with respect to the GPS satellites in view. These receiver-satellite clock offsets would then be shared with other platforms, allowing for a CVM solution for receiver-receiver clock offsets. The conceptual operating scenario involves the PPP and CVM applications executing in real-time and producing near real-time results. The issues of communicating information between platforms, the communication of precise estimates of orbit and clock solutions for the GPS satellites to the platforms, the extrapolation of near-real-time estimates, and the resolution of a CVM system bias are not here addressed.

The experiments were conducted in February and October 2007 using a mobile platform located at NSFD as one platform and the International Global Navigation Satellite System (GNSS) Service (IGS) reference site USN3 located at the United States Naval Observatory (USNO) as the second platform. The USN3 GPS receiver is an Ashtech Z12T that is directly referenced to UTC (USNO), the DoD Master Clock. Also, high-rate data (1-second interval) are available for postprocessing from USN3 via the Web site <ftp://cddis.gsfc.nasa.gov/gps/data/highrate/>. The mobile platform was a van equipped with GPS receivers, a rubidium oscillator that served the role of the platform clock, a portable cesium clock that served the role of representing the Master Clock at USNO, and a time-interval counter to compute the time differences between the rubidium oscillator and the portable cesium clock. All data were collected and postprocessed in a manner reflecting a real-time processing sequence. Altogether, data from 3 days of testing are presented. The platform positioning results demonstrated that the PPP accuracy was at the decimeter level. By using a Kalman filter approach to reduce the noise level and removing a system bias, the CVM results demonstrate that the receiver-receiver clock offsets can be determined to the 1-2 nanosecond level.

EXPERIMENT DESCRIPTION

HARDWARE DESCRIPTION

The conceptual setup of the experiment is shown in Figure 1. The principal components are a slam-synched GPS receiver (an Ashtech Z12T), a rubidium oscillator (Rb Oscillator, an SRS FS725 Rubidium Frequency Standard) that provides the reference 20 MHz carrier signal (via an amplifier, "Amp") and a one-pulse-per-second (1 PPS) signal to the Ashtech Z12T, another GPS receiver (an Ashtech Z12) that provided a 1 PPS signal that is used to steer the Rb oscillator and provided backup tracking data, a portable cesium clock (Cs Oscillator, an Agilent 5071A Cesium Frequency Standard) that provides a local representation of the USNO Master Clock, a time-interval counter (SRS SR620) that is used to measure the time difference in the 1 PPS signals generated by the Rb oscillator and the Cs oscillator, and a computer to record the data and provide a time stamp for the output from the time-interval counter. Note that the Z12T and Z12 shared the same dual-frequency antenna. These elements, along with supporting hardware, were arranged inside of a van with a GPS antenna mounted on the roof of the van and power provided by portable generators via UPS units, as shown in Figure 2.

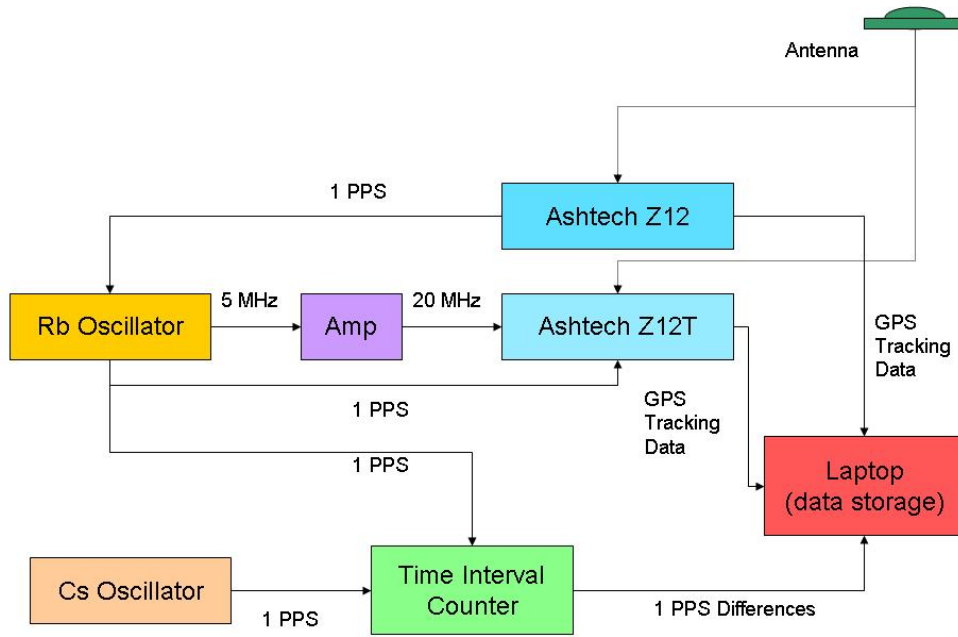


Figure 1. Conceptual experiment layout.



Figure 2. Van with experiment hardware.

TESTING DESCRIPTION

Tests were conducted during the weeks of 26 February-2 March and 1-5 October. The tests during February were set up to collect data while traveling from USNO to NSFD, at NSFD, and traveling back from NSFD to USNO. Analysis of the data indicated that obstructions (trees and buildings) prevented the collection of useful data between USNO and NSFD. However, the data collected on 27 February while at NSFD did not suffer from these obstructions. The tests on 2-5 October involved collecting data while traveling around NSFD. In general, only the data sets of 3 and 4 October were useful. Thus, there are 3 days of useful data available from these tests.

The portable cesium clock was used as a local representation of the USNO Master Clock for the purpose of computing the “true” time offset between the two platform clocks. The time offset of the portable cesium clock with the USNO Master Clock was measured at USNO at the beginning of each experiment span and then measured again at the end of the experiment span. It was assumed that the portable cesium would drift with a nearly constant frequency offset with respect to the Master Clock over the experiment span. This drift rate was taken to be the difference in the time offset measured before and after the experiment divided by the interval between these offset measurements. Thus, variations in the portable cesium clock beyond this frequency offset could not be accounted for in the CVM results, but these variations were assumed to be at or below the nanosecond level.

Once the equipment was assembled in the van and the generators started, the GPS receivers, the computer, the Rb oscillator, and time-interval counter were powered on. Note that the portable cesium clock has an internal battery, allowing movement between power sources while maintaining operating conditions, and was powered by the auxiliary power unit of the van until power from the portable generators was available. An initial warm-up period allowed the GPS receivers to complete acquisition of the GPS signals, allowed the Rb oscillator to lock on to the 1 PPS signal from the GPS receiver, and allowed for the computer to boot up and the data acquisition software used to collect the measurements from the time-interval counter and the software used to collect the GPS data to be initialized. The GPS receivers were configured to collect dual-frequency pseudorange and carrier-phase data at 1-second intervals. The data collection from the time-interval counter was configured for 1-second intervals as well. The clock on the computer was manually set to within a few seconds of the time provided by the portable cesium clock. After all of the equipment was operating normally and the data collection appeared to be in order, the van was driven over a closed loop pattern at NSFD. This particular loop was chosen to avoid obstructions (buildings and trees). A schematic of the loop is shown in Figure 3. A round trip on this loop was approximately 2 km. Speeds on this course reached approximately 25-30 miles per hour, although stops were required to obey traffic laws. This loop would be repeated for approximately 2 hours each day of testing. At the end of the testing period, the data were backed up and transferred to servers for storage, and the equipment powered off except for the portable cesium clock, which was transferred back to a laboratory to maintain a secure power source.

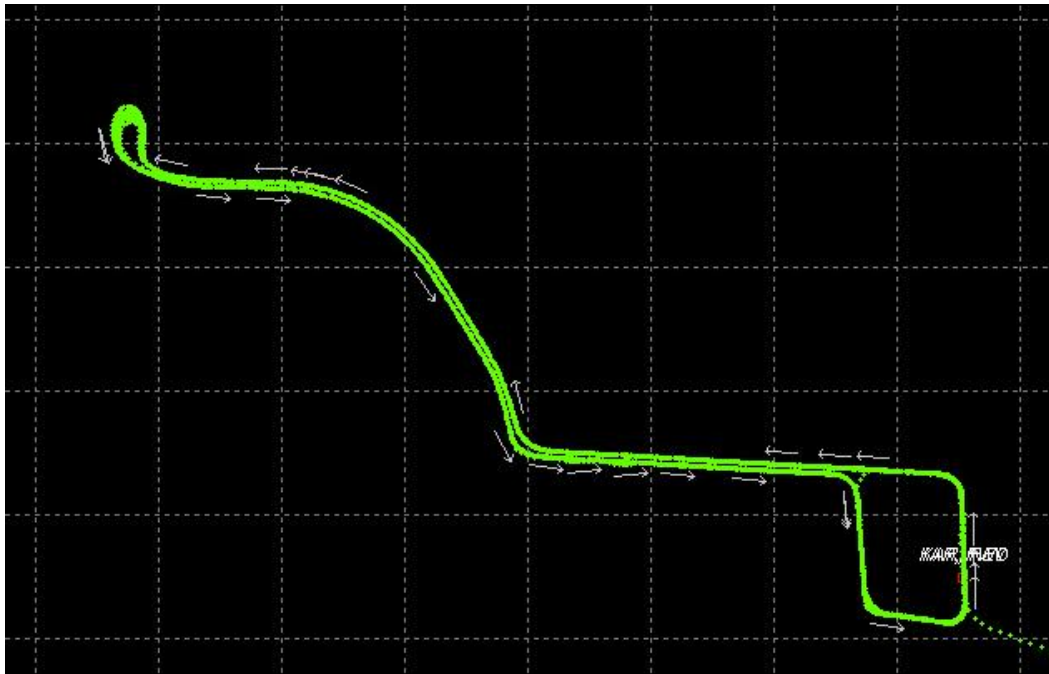


Figure 3. Experiment course (blocks are 100 meters on a side).

RESULTS

The data processing began with the acquisition of the GPS satellites' precise orbit and clock solutions from IGS and the National Geospatial-Intelligence Agency (NGA). The IGS solutions were computed at 15-minute intervals for the satellites' orbits and at 30-second intervals for the satellites' clock solutions. The NGA solutions were computed at 5-minute intervals for both the orbit and clock solutions. Using the broadcast satellite ephemeris data, a trajectory solution for the van was computed using a short-baseline kinematic baseline technique referenced to a surveyed site as NSFD. Using the IGS precise orbit and clock solutions, a trajectory solution for the van was computed using a precise point positioning (PPP) technique. These trajectory solutions were computed once using the data from the Ashtech Z12 receiver and again using the data from the Ashtech Z12T receiver, which was the basis for computing the receiver-receiver time offsets. The various van trajectory solutions were repeated using the NGA orbit and clock solutions. For a specific set of receiver and precise orbit and clock data sets, the trajectories from both solution techniques were differenced in the north, east, and up directions to evaluate the quality of the PPP solutions under the assumption that the short-baseline kinematic technique should provide solutions with accuracies of less than 10 cm. Figures 4 and 5 show the results of these trajectory differences for the test on 3 October using the Ashtech Z12 data set and the Ashtech Z12T data set, respectively, in conjunction with the IGS satellite orbit and clock solutions. The trajectory results of 3 October are representative of all 3 days of testing.

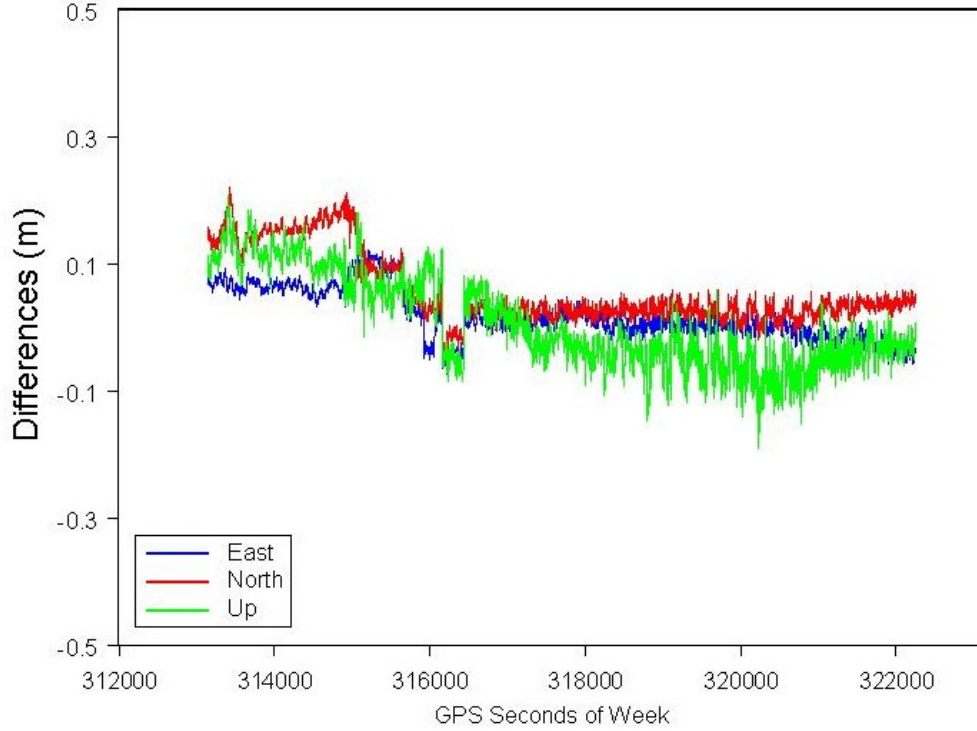


Figure 4. 3 October trajectory solution differences (meters) between the PPP and the short-baseline kinematic solutions using the Ashtech Z12 data and the IGS GPS precise orbit and clock solutions.

The next step in the data processing began with the collection of the GPS high-rate data (1-second interval) from USN3 in RINEX format that corresponded to each testing period. Using the GPS ephemeris information (from either the broadcast ephemeris message or the precise orbit information) and the van's trajectory solution, the relative clock offset between the a receiver's clock and a satellite clock can be computed as

$$\left(\Delta t_j - \Delta t^i\right)_k = \frac{1}{c} \left(p_{j,k}^i - \rho_j^i - I_j^i - T_j^i - \varepsilon_j^i \right) \quad (1)$$

where Δt is the time offset of the transmitter/receiver clock with respect to a reference time system (e.g. GPS Time), $p_{j,k}^i$ represents the pseudorange measurement between GPS satellite i and the receiver j at frequency (L1 or L2) k , ρ_j^i represents the geometric range and is computed using the known satellite and station position information, I represents the ionospheric effect on the pseudorange measurement, T represents the tropospheric effect, ε represents the remaining pseudorange measurement error sources, and c is the speed of light. The common-view mode technique computes the time offset between receiver clocks by differencing the receiver-satellite clock differences that involve the same satellite, i.e.

$$\left(\Delta t_{USN3} - \Delta t_{van}\right)_i \cong \left(\Delta t_{USN3} - \Delta t^i\right) - \left(\Delta t_{van} - \Delta t^i\right) \quad (2)$$

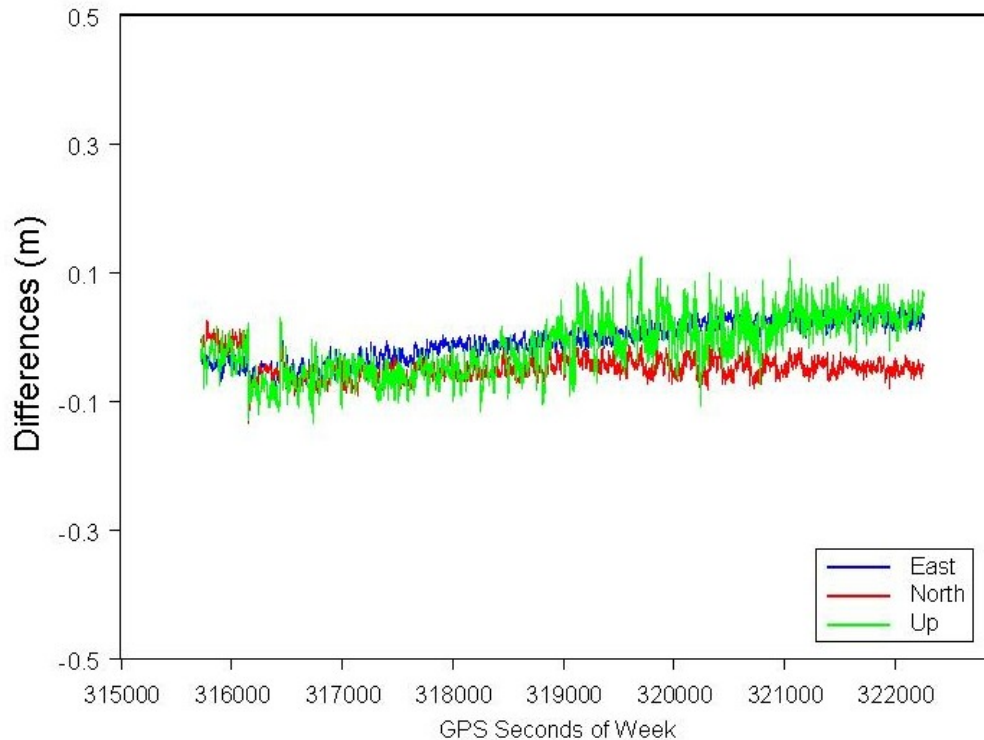


Figure 5. 3 October trajectory solution differences (meters) between the PPP and the short-baseline kinematic solutions using the Ashtech Z12T data and the IGS GPS precise orbit and clock solutions.

Figure 6 shows the receiver-receiver clock offsets for 3 October using the L1 pseudorange measurements (P1) without correcting for ionospheric or tropospheric effects. The legend notation of P1D i indicates that differences involve the GPS satellite with PRN i . Note that the approximately 250-nanosecond bias in these differences represent the overall system bias due to the arrangement of the equipment in the experiment. Note that the variation in the relative time offset from a single satellite ranges from 20-40 nanoseconds.

The next step in the data processing involved using the measurements of receiver-receiver time offsets of Eq. (2) as measurements in a single-state Kalman filter to form an estimate of the receiver-receiver clock offset. The initial value of the estimated relative clock offset is determined by using all measurements at an epoch to compute a mean value and standard deviation about the mean. If the standard deviation is within a predefined threshold, the initial estimate is set equal to the mean and the associated covariance is set equal to the measurement variance. If the standard deviation is not less than the predefined threshold, the measurement with the largest difference with respect to the mean is discarded and the mean and standard deviation are recomputed. This process is iterated until either the predefined threshold on the standard deviation is achieved or there are only three measurements left. If the latter condition occurs, the epoch is rejected and the next epoch is inspected. The process of rejecting measurements was adopted because the initialization was typically attempted near the beginning of the data collection period during which some pseudorange measurements were the first values recorded for a particular satellite and could experience significant errors. Once the initial estimate of the relative clock offset was formed, it would be propagated to the next measurement epoch as a constant value to form the *a priori* estimate and, to compensate for this assumption, process noise would be added to the covariance propagation. The *a posteriori* estimate at the next epoch would be formed by incorporating all the measurements that passed

a simple editing test. The editing test was based on the residual between the current estimate and the measurement. If the absolute value of the residual was greater than a maximum threshold or was greater than five times the current covariance, the measurement was rejected. Figure 7 shows the filter results after processing the measurements shown in Figure 6 along with the mean clock offset at each epoch and a linear fit for reference. Note that variability in the epoch mean is much smaller than the measurements in Figure 6 and the filtered estimate variability is much smaller than the epoch mean, as might be expected.

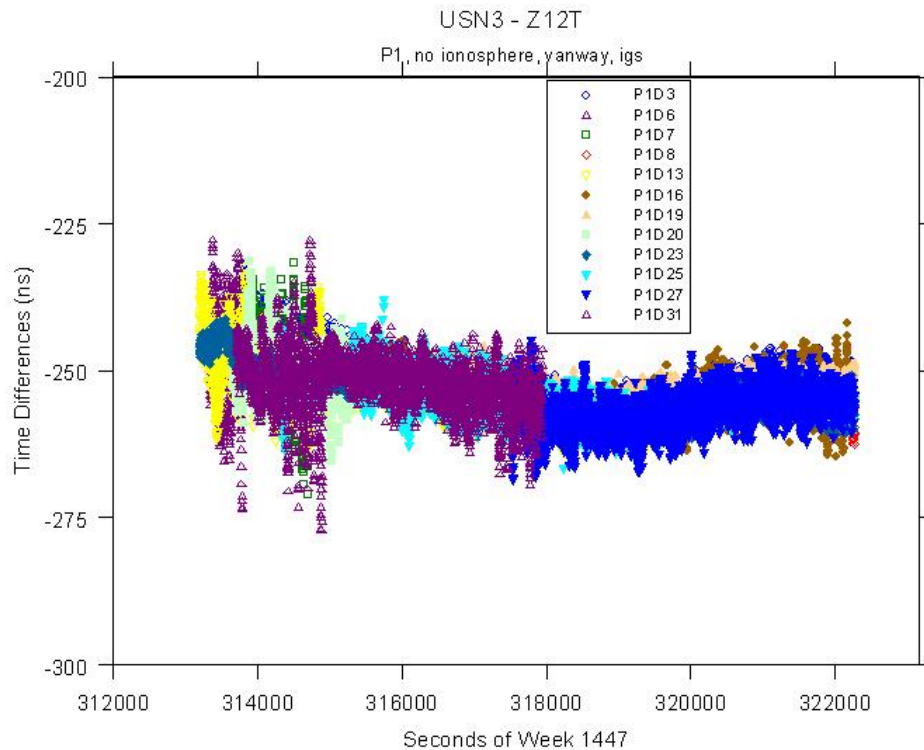


Figure 6. Time offsets from Equation (2) between USN3 and the mobile platform on 3 October using L1 pseudorange measurements without tropospheric and ionospheric corrections where P1Di correspond to PRN i.

The final step in the data processing involves differencing the estimated time offsets from the offsets measured by the time-interval counter and removing a bias from these differences. The variance of the adjusted differences is then used as one measure of the quality for this procedure. The estimated clock offsets and the resulting adjusted differences are shown in the following subsection.

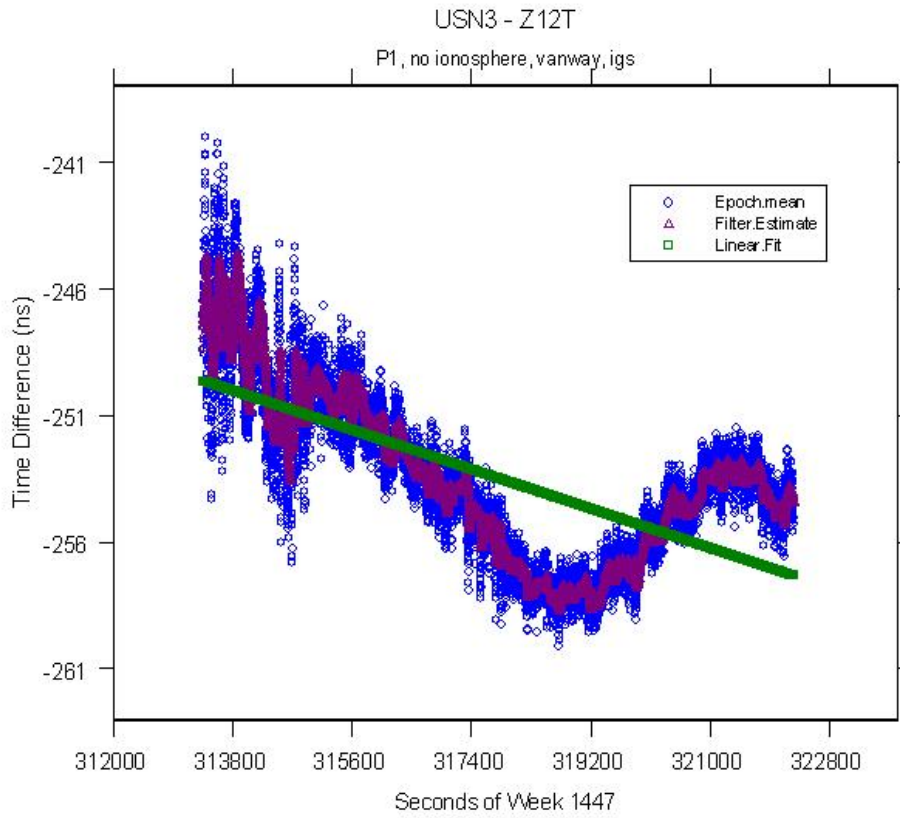
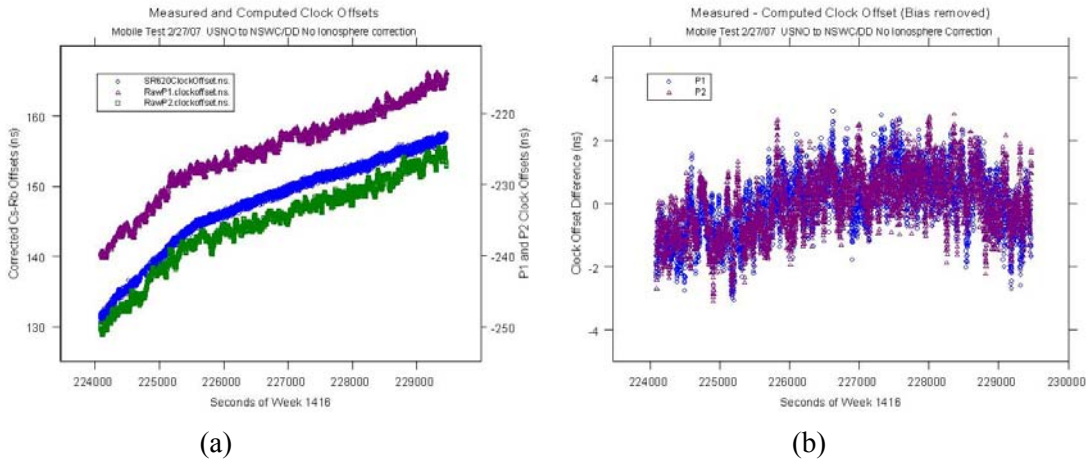


Figure 7. Filter and epoch mean values for the time offsets of Figure 6.

27 FEBRUARY TEST

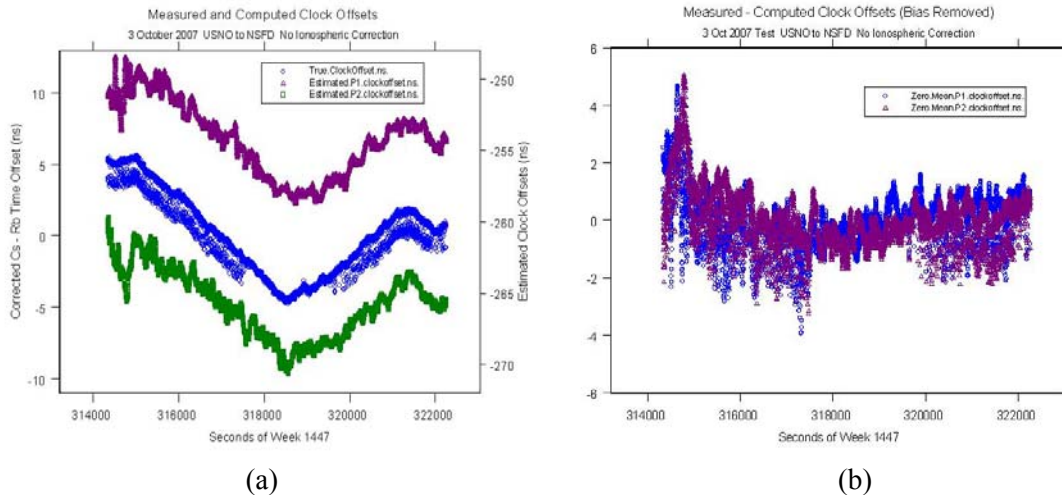
The results for the test conducted on 27 February 2007 (GPS week 1416) are shown in Figures 8. The data span is 90 minutes with a total relative clock change of nearly 30 nanoseconds. Note that there is a change in the relative drift rate at about 225500 seconds of week, which is probably due to the steering of the rubidium oscillator. The estimated time offsets using the pseudorange measurements track this change as seen in Figure 8a. Biases of 373.2 nanoseconds and 384.9 nanoseconds were removed from the differences between the measured offset and the L1- and L2-based estimated offsets to produce the results in Figure 8b. These time offset differences are in the range of -2 to $+2$ nanoseconds and have standard deviations of 0.77 and 0.76 nanoseconds, respectively.



Figures 8. (a) Measured and computed clock offsets for 27 February 2007 and (b) differences between the measured and computed clock offsets after removing biases.

3 OCTOBER TEST

The results for the test conducted on 3 October 2007 (GPS week 1447) are shown in Figures 9. The data span is 132 minutes with a total relative clock change of approximately 10 nanoseconds. Note that there are four major inflection points in the relative clock offset due to the steering of the rubidium oscillator. The first occurs near the beginning of the data at approximately 315000 seconds of week, the second occurs near the midpoint of the data span at approximately 318500 seconds of week, and the remaining two occur near the end of the data span at approximately 321500 and 322000 seconds of week. The estimated time offsets using the pseudorange measurements track these changes, as seen in Figure 9a. Note that the measured time offsets curve (blue, middle curve) has spurious points separated by approximately 1 nanosecond from the remainder of the data for the first portion of the time span and again towards the end of the time span. The origin of these data is unknown, although it is suspected that it may be due to the behavior of the time-interval counter. Biases of 254.2 nanoseconds and 265.8 nanoseconds were removed from the differences between the measured offset and the L1- and L2-based estimated offsets to produce the results in Figure 10b. These time-offset differences are generally in the range of -2 to $+2$ nanoseconds, with some larger differences occurring near the beginning of the data span and for some portions where the spurious measured time offsets occur. The time offset differences in Figure 8b have standard deviations of 0.92 and 1.0 nanoseconds, respectively. The larger values of the standard deviations compared to those of 27 February are related to the spurious measured time offsets.



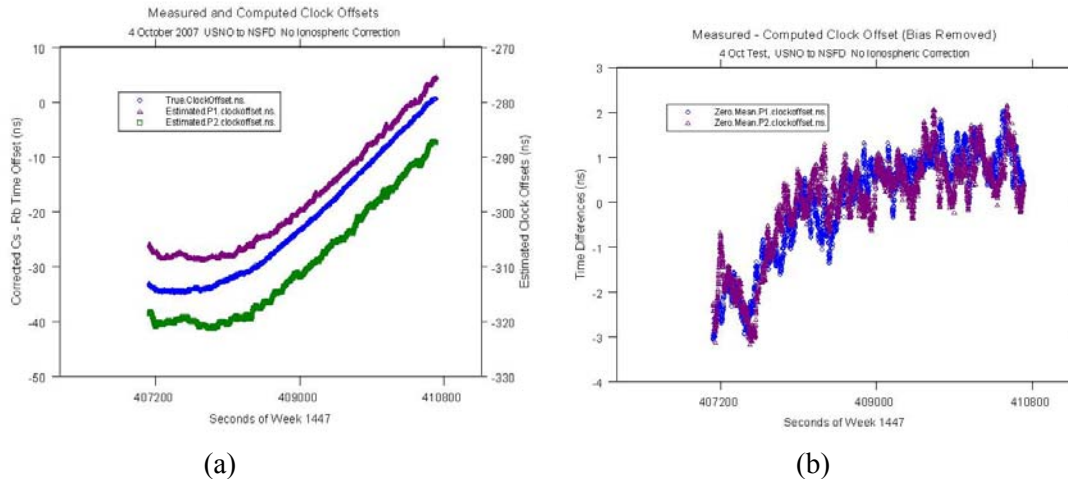
Figures 9. (a) Measured and computed clock offsets for 3 October 2007 and (b) differences between the measured and computed clock offsets after removing biases.

4 OCTOBER TEST

The results for the test conducted on 4 October 2007 (GPS week 1447) are shown in Figures 10. The data span is 60 minutes, with a total relative clock change of approximately 35 nanoseconds. Note that there are no major inflection points in the relative clock offset, but rather a smooth change in the relative clock rate near the beginning of the data interval due to the steering of the rubidium oscillator. The estimated time offsets using the pseudorange measurements track the trend of the measured clock offset, as seen in Figure 10a. Biases of 275.7 nanoseconds and 287.6 nanoseconds were removed from the differences between the measured offset and the L1- and L2-based estimated offsets to produce the results in Figure 10b. These time offset differences are generally in the range of -2 to $+2$ nanoseconds, with some larger differences occurring near the beginning of the data. The time offset differences in Figure 10b have standard deviations of 1.2 and 1.1 nanoseconds, respectively. The larger values of the standard deviations relative to those of 27 February are related to the differences during the early portion of the data span.

CONCLUSIONS

Two experiments conducted over 3 days during February and October 2007 demonstrate the possibility of achieving relative real-time time synchronization at the few-nanosecond level between two mobile clocks. This level of synchronization is based upon using GPS data with a loosely coupled relationship between a precise point positioning (PPP) technique and the common view mode (CVM) technique. The simulated real-time offsets are estimated using a single-state Kalman filter with errors on the order of ± 2 nanoseconds and standard deviations on the order of 1 nanosecond. For this approach to be applicable in an operational scenario, other real-time issues need to be resolved, including the generation and transfer of precise GPS satellite orbit and clock solutions to support the PPP technique that is the core element of this approach, the extrapolation of the clock offset estimates to mitigate any latency issues in the support of real-time support of other systems, and a calibration process to remove a system bias.



Figures 10. (a) Measured and computed clock offsets for 4 October 2007 and (b) differences between the measured and computed clock offsets after removing biases.

ACKNOWLEDGMENTS

This project was funded under the Discretionary Technical Investment Program (DTIP) at the Naval Surface Warfare Center Dahlgren Division. The authors would like to thank Mr. Larry Triola for his guidance and support under the DTIP. The authors would also like to recognize the contributions of several individuals that helped to make these experiments possible. Dr. Ed Powers of the United States Naval Observatory (USNO) arranged for the loan of the Ashtech Z12T with supporting amplifier and the portable cesium clock. He also provided advice and suggestions that helped in carrying out the experiment. Mr. Chris Law of NSWC Dahlgren provided invaluable logistical support. Mr. Andrew Sutter of NSWC Dahlgren helped in processing the data collected and providing the truth and PPP trajectory solutions for the van.

REFERENCES

- [1] L. Colombo, A. W. Sutter, and A. G. Evans, 2004, "Evaluation of Precise , Kinematic GPS Point Positioning," in Proceedings of the ION GPS GNSS 2004 Meeting, 21-24 September 2004, Long Beach, California, USA (Institute of Navigation, Alexandria, Virginia), pp. 1423-1430.
- [2] A. Sutter, A. Evans, J. Cunningham, J. Saffel, and O. Colombo, 2007, "Evaluation of Dynamic Precise Point Positioning Using NGA Post-Fit GPS Satellite Orbits and Clocks at 5-Minute Interval" (FOUO), presented at the Joint Navigation Conference, 2-6 April 2007, Orlando, Florida, USA.
- [3] B. W. Parkinson and J. J. Spilker, 1996, **Global Positioning System: Theory and Applications, Vol. II** (American Institute of Aeronautics and Astronautics, Reston, Virginia), pp. 490-498.